

The feasibility of 1-stop examination of coronary CT angiography and abdominal enhanced CT

Wei Fang, MD, Cai-Hong Wang, MD, Yi-Fan Yu, MD, Li-Huan Wang, MD, Dan-Hua Tang, MD, Da-Bo Xu, MD, Zuo-Yun Ding, MD, Wen-Hao Gu, MD*

Abstract

This study aims to evaluate the feasibility of performing coronary computed tomography angiography (CCTA) and abdominal enhanced computed tomography (CT) with 1-time injection of the agent.

CCTA images (right coronary artery, left anterior descending coronary artery, and left circumflex coronary artery) were collected from 20 patients who completed a 1-stop combined examination of CCTA and abdominal enhanced CT (group A), 20 patients who only underwent abdominal enhanced CT (group B1), and 20 patients who only underwent CCTA (group B2). These images were interpreted using the 5-point Likert scale system by 2 experienced radiologists, and abdominal images were observed for breathing artifact. CT value, signal-to-noise ratio (SNR), and CTDI were recorded and compare among the 3 groups.

The difference in image quality of the coronary and total volume of the contrast agent between group A and group B1 was not statistical significant ($P > .05$). The CT value and SNR in group B1 (CCTA) (CT: 394.65 ± 59.23 , SNR: 17.38 ± 4.13) increased, compare with Group A (CT: 360.35 ± 34.16 , SNR: 13.76 ± 1.84 , $P = .03$, $.01$), while CTDI was undifferentiated between group A (17.14 ± 6.20) and group B1 (18.38 ± 9.79) ($P = .64$). The difference in CT value and SNR at the arterial phase and CT value at the venous phase between group A (abdomen) and group B2 were statistically significant, the CTDI in group A (9.09 ± 1.05) increased, compared with group B2 (8.23 ± 1.33) ($P = .03$), and SNR at the venous phase in group B2 (12.50 ± 2.43) increased, compared with group A (10.89 ± 2.03) ($P = .03$).

Revolution CT can capture full images and very rapidly switch to the scan mode, enabling a 1-stop axial CCTA and enhanced helical abdominal scan. The 1-stop combined scan resulted in a satisfactory image quality, which reduced the contrast agent dose and simplified the workflow.

The 1-stop combined scan allows for the high success rate of the examination, reduces the number of examinations, and decreases the dose and risk of injection of the contrast agent. This would be helpful for patients to obtain diagnostic images in time.

Abbreviations: ASIR = adaptive statistical iterative reconstruction technique, BMI = body mass index, CAD = coronary artery disease, CCTA = coronary CT angiography, CPR = curved planar reconstruction, CT = computed tomography, LAD = left anterior descending coronary artery, LCX = left circumflex coronary artery, MDCT = multidetector CT, MIP = maximum intensity projection, RCA = right coronary artery, ROI = region of interest, SNR = signal-to-noise ratio, VR = volume rendering.

Keywords: abdominal enhanced CT, coronary CT angiography, spiral computed, tomography

1. Introduction

Coronary artery disease (CAD) has been well-recognized as an important cause of death worldwide.^[1-3] It is of great significance to reduce the mortality and improve the prognosis

of CAD patients through the use of imaging methods, in order to comprehensively and accurately evaluate the coronary artery, and achieve its early detection and intervention. In recent years, with great progress in the hardware, software, and imaging postprocessing technology of computed tomography (CT),^[4-6] the success rate and image quality of coronary CT angiography (CCTA) have been continuously improved and have become an important means of clinical diagnosis and postoperative evaluation in CAD.^[7-9] The abdomen is the “hardest hit” by the disease due to its multiple organs. Therefore, many patients require simultaneous CCTA and contrast-enhanced abdominal CT. Traditional CT checks 2 times. This not only induces the overdose of iodine and increased risk of injection, but also brings about long inspection durations and high cost. Reducing the amount of iodine contrast agents and the burden of patients with the premise of completing the joint scanning of multiple parts of the body with high quality in 1 station has become a hot topic in the field of imaging in recent years.^[10-18] The 256-multidetector CT (MDCT) is equipped with a 16-cm wide-bodied detector, which makes it possible for a 1-stop multisite joint scan to become a reality. In the present study, 256-MDCT was used to perform a combined scan of CCTA and contrast-enhanced abdominal CT. These were compared with single-site contrast-enhanced CT to analyze the advantages of a 1-stop scan using

Editor: Heye Zhang.

WF and CHW contributed equally to this article

Jiangsu Taicang city science and technology project—key research and development plan (development of society) (No TC2017SFYL03).

The authors have no conflicts of interest to disclose.

Department of Radiology, Taicang City First People's Hospital Affiliated to Suzhou University, Suzhou, China.

* Correspondence: Wen-Hao Gu, Department of Radiology, Taicang City First People's Hospital Affiliated to Suzhou University, No. 58 of Changsheng South Road, Taicang City, Suzhou 215400, China (e-mail: gu_docwh08@163.com).

Copyright © 2018 the Author(s). Published by Wolters Kluwer Health, Inc. This is an open access article distributed under the terms of the Creative Commons Attribution-Non Commercial-No Derivatives License 4.0 (CCBY-NC-ND), where it is permissible to download and share the work provided it is properly cited. The work cannot be changed in any way or used commercially without permission from the journal.

Medicine (2018) 97:32(e11651)

Received: 30 March 2018 / Accepted: 28 June 2018

<http://dx.doi.org/10.1097/MD.0000000000011651>

256-MDCT in coronary angiography combined with contrast-enhanced abdominal scan.

2. Materials and methods

2.1. Subjects

A total of 20 patients who underwent coronary combined with abdominal enhanced scanning in the First People's Hospital of Taicang from January 2017 to June 2017 were enrolled into this study. In addition, 20 patients who underwent abdominal scans and 20 patients who underwent coronary scans were enrolled into the study. Among these 60 patients, 38 patients were males and 22 patients were females. The age of these patients ranged within 28 to 84 years old, and their average age was 59.7 ± 11.0 years old. Inclusion criteria: patients without contraindications and allergic history of iodinated contrast agent, patients without a history of severe hepatic and renal dysfunction, and patients without a history of severe cardiac insufficiency. This study was conducted with approval from the Ethics Committee of Taicang city first people's hospital affiliated to Suzhou University. All patients provided a signed informed consent.

2.2. Inspection methods: The inspection equipment used in the present study was 256-MDCT (Revolution CT, GE Healthcare, Milwaukee, Wisconsin)

Single contrast-enhanced abdominal scan scheme: Scanning range was from 10 mm above the diaphragmatic surface to the lower edge of the kidney, voltage was 120 kV, and ampere was automatic mA (range: 200–500 mA). Noise Index (NI) was set at 9, detector width was 80 mm, pitch was 0.992, and the speed of the CT tube was 0.28 seconds. The scanning mode was spiral scan, and standard reconstruction algorithm was employed (adaptive statistical iterative reconstruction technique [ASIR]-V20%). Reconstruction slice thickness was 5.0 mm, gap was 5.0 mm, window width was 350, and window level was 50. Contrast medium administration scheme: 350 mg I/mL of iohexol was used, the total dose was 90 mL, and the injection rate was 3 to 5 mL/s. Subsequently, 30 mL of normal saline was injected. Inspection methods: The abdominal aorta was traced by automatic triggering region of interest (ROI) tracing, and the trigger threshold was 150 HU. At 0.9 seconds after reaching the threshold (breathing instructions, the patient was instructed to hold their breath), arterial phase scanning was performed. Then, venous phase scanning was performed after 40 seconds.

Scanning plan of single coronary artery imaging: The scan range was from the lower edge of the tracheal carina to the bottom of the heart. Automated tube potential selection (kV Assist) and automatic Smart mA (range: 200–650 mA) were adopted. NI was set at 22, detector width was 140 to 160 mm, and the speed of CT tube was 0.28 seconds. The scanning mode was axial scan, and the soft tissue reconstruction algorithm was employed (ASIR-V50%). Reconstruction slice thickness was 0.625 mm, window width was 800, and window level was 100. Contrast medium administration scheme: 350 mg I/mL of iohexol was used, and individualized administration was performed. The administration rate was 26.25 mg I/kg per s, and the plateau phase of administration was 9 seconds. Subsequently, 30 mL of normal saline was injected. Inspection methods: autogating was used to record and analyze the heart rate of patients, which automatically recommended the appropriate scan scheme. The aortic root was traced by automatic triggering ROI tracing,

where the trigger threshold was 250 HU. At 2 seconds after reaching the threshold, the scan was triggered. During the whole process, the patient was in the state of free breathing. After completion of the inspection, the appropriate phase images were selected for coronary surface reconstruction and volume rendering (VR).

Combined scan scheme: The scan range included the chest and abdomen. Plane 1 was a nonenhanced abdominal scan (it was the same with the single abdominal scan), and Plane 2 was a coronary axial scan (it was the same with the single coronary scan). This was rapidly switched to spiral scan mode after the end of the scan, with a switching time of 1.7 seconds. Then, Plane 3 abdominal arterial phase scanning was performed, and venous phase scans were performed after 40 seconds. Administration mode of contrast agent: 350 mg I/mL of iohexol was used, and the total dose was 90 mL. The dose of the drug required for the coronary axial scan was calculated according to the individualized administration scheme (26.25 mg I/kg per s [body weight], for 9 seconds). After the end of the injection, the remaining contrast agent was immediately injected at a rate of 4 mL/s, and 30 mL of normal saline was additionally injected. During the whole scan, the patients were kept in a free breathing state.

2.3. Image processing

Abdominal images were reconstructed according to a slice thickness of 5 mm and a gap of 5 mm. Standard algorithm was employed (ASIR-V20%). Window width was 350, and window level was 50. A group of images on a certain phase that could well display the 3 coronary arteries were selected for thin-slice reconstruction. The slice thickness was 0.625 mm. Soft tissue reconstruction algorithm was employed (ASIR-V50%). Window width was 800, and window level was 100. The Auto Coronary Analysis tool in Advantage Workstation 4.6 (ADW4.6, GE Healthcare, Milwaukee, Wisconsin) was used for the postprocessing of images. The postprocessing methods mainly included the following: curved planar reconstruction, multiplanar reconstruction, VR, and maximum intensity projection ROI VR.

2.4. Image quality scores and analysis

All images were independently interpreted using the double-blind method by 2 senior attending physicians with rich experience in coronary diagnosis. The coronary images were subjectively scored based on the right coronary artery (RCA), left anterior descending coronary artery (LAD), and left circumflex coronary artery (LCX). The 5-point scoring system for the image quality of each coronary artery^[19]: with the presence of a motion artifact in each coronary artery as a scoring standard (1–5 points), 5 points indicate no motion artifact, 4 points indicate slight motion artifact, and 3 points indicate mild motion artifacts (these can be used for diagnosis); 2 points and 1 point indicate obvious and severe motion artifacts, respectively (these cannot be used for diagnosis). In patients with 1 point, vascular split-level was severe, severe blurred shadows were present around the vessels, and it was difficult to distinguish blood vessels from its surrounding tissues. This cannot be used for diagnosis. In patients with 2 points, severe blurred shadows could be observed around the blood vessels. This cannot be used for diagnosis. In patients with 3 points, slight blurred shadows could be observed around the blood vessels, and the development of the lumen was good. This can be used for diagnosis. In patients with 4 points, vascular split-level was not obvious, the distributions were

Table 1
Evaluation of the general condition ($\bar{x} \pm s$).

Group	Age	BMI	Heart rate	Age	BMI
A	62.00±10.47	25.59±1.88	59.98±20.13	62.00±10.47	25.59±1.88
B1	58.20±9.70	25.70±2.17	65.55±9.46	—	—
B2	—	—	—	58.95±13.22	23.17±2.93
<i>t</i>	1.19	-0.16	-1.12	0.80	3.11
<i>P</i>	.24	.87	.27	.42	.004

BMI = body mass index.

relatively continuous, and slightly blurred shadows were present around the vessels. This can be well used for diagnosis. In patients with 5 points, the edges of the vessels were sharp, there was no split-level artifact, and the distributions were continuous. This can be used for definite diagnosis.

2.5. Statistical analysis

Data were statistically analyzed using statistical software SPSS 19.0. The homogeneity of the subjective scores of image quality provided by the 2 physicians was analyzed using kappa test, where $\kappa > 0.75$ was considered highly homogeneous. The mean values and standard deviations (SDs) of CT, signal-to-noise ratio (SNR), and CTDI values of images in the 3 groups were analyzed and calculated; the obtained measured data were expressed as mean \pm SD ($\bar{X} \pm SD$), and these were evaluated using independent sample *t* test. *P* < .05 was considered statistically significant.

3. Results

3.1. Evaluation of the general condition

The difference in age among these 3 groups was not statistically significant (*P* > .05). The difference in body mass index (BMI) between group A and group B1 was not statistically significant. BMI was higher in group A (25.59±1.88) than in group B2 (23.17±2.93). The difference in heart rate between group A and group B1 was not statistically significant (Table 1).

3.2. Analysis of objective data

The CT and SNR values were higher in group B1 (CT: 394.65 ± 59.23, SNR: 17.38 ± 4.13) than in group A (CT: 360.35 ± 34.16, SNR: 13.76 ± 1.84) (*P* = .03 and .01). The differences in arterial phase CT value, SNR value, and venous phase CT value between group A and group B2 were not statistically significant (*P* > .05), and the venous phase SNR value was higher in group B2 (12.50 ± 2.43) than in group A (10.89 ± 2.03) (Table 2).

Table 2
Image quality assessment table ($\bar{x} \pm s$).

Group	Aortic root			Abdominal aorta			Main trunk of portal vein	
	CT value	SNR	CTDI	CT value	SNR	CTDI	CT value	SNR
A	360.35±34.16	13.76±1.84	18.38±9.79	373.28±41.51	26.76±4.09	9.09±1.05	143.83±13.89	10.89±2.03
B1	394.65±59.23	17.38±4.13	17.14±6.20	—	—	—	—	—
B2	—	—	—	358.50±78.27	28.26±7.82	8.23±1.33	152.18±19.81	12.50±2.43
<i>t</i>	-2.24	-3.58	0.48	0.75	-0.76	2.27	-1.56	-2.28
<i>P</i>	.03	.01	.64	.46	.45	.03	.13	.03

CT = computed tomography, SNR = signal-to-noise ratio, CTDI = CT dose index.

Table 3
Subjective image quality assessment form of coronary artery ($\bar{x} \pm s$).

Group	RCA	LAD	LCX	Contrast agent dosage
A	3.60±0.82	3.95±0.60	3.95±0.60	46.07±6.08
B1	3.70±0.66	3.70±0.57	4.00±0.65	47.35±5.47
<i>t</i>	-0.47	1.31	-0.25	-0.70
<i>P</i>	.64	.19	.80	.49

LAD = left anterior descending coronary artery, LCX = left circumflex coronary artery, RCA = right coronary artery.

3.3. Image quality scores

The quality of images in groups A and B1 met the requirements of diagnostic imaging (≥ 3). The homogeneity of all data provided by the 2 physicians was good ($\kappa = 0.83$). The differences in quality scores among images of RCA, LAD, and LCX were not statistically significant (*P* > .05, Table 3). There was no respiratory artifact in the subjective evaluation of enhanced abdominal images. Hence, this could be well used for diagnosis (Figs. 1–3).

3.4. Evaluation of radiation dose

The differences in CTDI and DLP values between group A and group B1 were not statistically significant (*P* = .64 and *P* = .71). The CTDI value was higher in group A (9.09±1.05) than in group B2 (8.23±1.33) (*P* = .03, Table 2).

4. Discussion

With the continuous update and development of CT technology and equipment, CCTA has been widely applied in clinic. Compared with DSA and cardiac ultrasound, CT has the advantages of quickness, convenience, noninvasion, and high specificity. Therefore, it has gradually become the first choice for coronary heart disease screening and the postoperative evaluation of coronary stent implantation.^[20–24] However, many patients go to hospital for examination due to more than 1 factor. A large number of patients need to undergo simultaneous enhanced abdominal CT scans based on CCTA. Traditional enhanced CT requires several checks, and patients are injected twice in the CT room, causing the dose of the contrast agent to be high. Single axial scanning using a 16-cm wide-bodied detector in Revolution CT can cover the heart, liver, and other organs.^[25–26] In addition, the speed of the tube is only 0.28 s/r, and the snapshot freeze in coronary angiography and the ASIR greatly improve the temporal resolution of CT images.^[27–29] Thus, under the precondition of a single injection of contrast agents, there would



Figure 1. Coronary artery images for combined scanning. Images of the same patient undergoing combined scanning are shown (male, 71 years old). (A–C) The LCX, LAD, and RCA of this patient are shown. The quality of the image is good, and the scores were 5, 4, and 4 points, respectively. LAD = left anterior descending coronary artery, LCX = left circumflex coronary artery, RCA = right coronary artery.



Figure 2. Abdominal images for combined scanning. (A, B) The sagittal and coronal images of the abdomen of a patient are shown. There was no respiratory artifact on the images, which meet the diagnostic requirements.

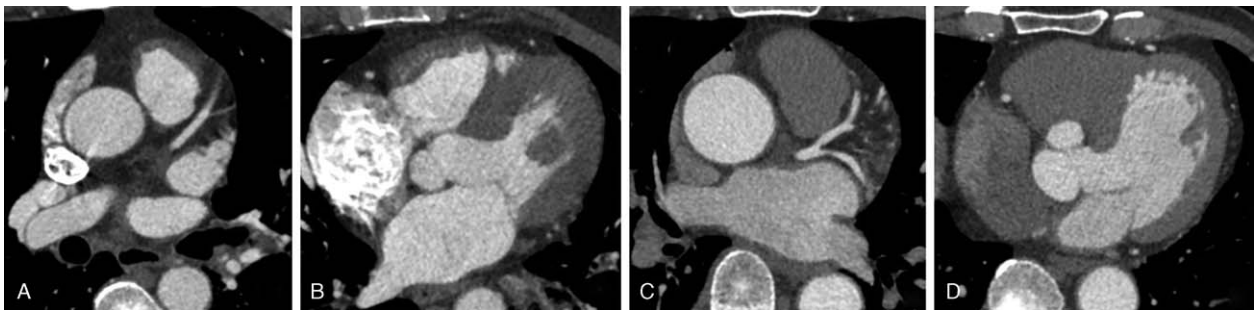


Figure 3. Coronary axial images. (A, B) Coronary axial images for combined scanning are shown. The radial artifacts produced by the dense contrast agent in the superior vena cava could be observed. This may affect the signal-to-noise ratio of the coronary artery images. (C, D) The axial images in single coronary scanning are shown. After dilution by normal saline (NS, 0.9% sodium chloride in water), no artifact was found in the superior vena cava.

be enough time to complete the abdominal scan after coronary angiography. This would effectively reduce the dose of the contrast agent, save on inspection cost, and reduce contrast agent-related side effects and potential risks. The objective of the present study was to attempt to combine CCTA and contrast-enhanced abdominal CT scans using Revolution CT, compare the results with those of the single-site enhanced CT, and analyze the advantages of Revolution CT 1-stop scanning in coronary angiography combined with enhanced abdominal scan.

The results of the present study revealed that the difference in image quality scores of coronary arteries between these 2 groups was not statistically significant. These results reveal that images obtained by combined scanning meet the diagnostic requirements. Causes for lower CT and SNR values compared with single coronary imaging: during the single coronary scan, the patient was injected with 30 mL of normal saline after individualized administration, in order to dilute the contrast agent in the superior vena cava. For the combined scan, an arterial phase abdominal scan was immediately performed after coronary imaging, no normal saline was injected for dilution, the contrast agent in the superior vena cava was thicker, and the formed radial artifact affected the measurement of CT and SNR values in the adjacent aorta. Differences in the measured CT and SNR values of the abdominal aorta and portal vein CT value were not statistically significant. The reason for this is that the difference in BMI induced the CTDI value in the single enhanced abdominal scan to be lower than that of the combined scan. The SNR during the portal phase scan in the single enhanced abdominal scan was higher than that of the combined scan. The reason may be that there was a time interval between continuous administrations during the combined scan, and the density of the intravascular bolus injection was not as high as that of the single abdominal scan.

Advantages of the present study: CCTA scanning could be rapidly performed and has high success rate. It can complete the whole scanning of the heart in 1 heartbeat cycle, there is no respiratory artifact on the images when combined with enhanced abdominal scan, and the subjective and objective data of images in these 3 groups were equivalent. This could all meet diagnostic requirements, and had high clinical feasibility. The coronary and abdominal enhanced images could be obtained with only 1 injection of the contrast agent. Hence, the dose of the contrast agent was reduced, and inspection cost and time were saved.

The deficiencies of the present study: The sample size was small. Hence, there is a need to further accumulate cases to confirm the reliability of this study. This study focused on image quality, and did not evaluate the influence of circulatory system diseases, primary heart diseases, and changes after intervention on imaging quality.

In summary, the scanning mode can be quickly switched during the scan using Revolution CT, due to its rapid response and wide-bodied characteristics. Therefore, the combined scanning of CCTA and enhanced abdominal CT can be completed in 1 station. This allows for the high success rate of the examination, reduces the number of examinations, and decreases the dose and risk of injection of the contrast agent. This would be helpful for patients to obtain diagnostic images in time.

Acknowledgment

The authors are particularly grateful to all the people who have given us help on this article.

Author contributions

Conceptualization: Wei Fang, Yi-Fan Yu, Li-Huan Wang, Dan-Hua Tang, Cai-Hong Wang, Da-Bo Xu, Zuo-Yun Ding, Wen-Hao Gu.

Data curation: Wei Fang, Yi-Fan Yu, Li-Huan Wang, Dan-Hua Tang, Cai-Hong Wang, Da-Bo Xu, Zuo-Yun Ding, Wen-Hao Gu.

Formal analysis: Wen-Hao Gu.

Funding acquisition: Wen-Hao Gu.

Methodology: Yi-Fan Yu, Li-Huan Wang, Wen-Hao Gu.

Writing – original draft: Wei Fang, Li-Huan Wang, Wen-Hao Gu.

Writing – review and editing: Wei Fang, Wen-Hao Gu.

References

- [1] Roberts R. Genetics of coronary artery disease. *Circ Res* 2014; 114:1890–903.
- [2] Rosendorff C, Lackland DT, Allison M, et al. Treatment of hypertension in patients with coronary artery disease: a scientific statement from the American Heart Association, American College of Cardiology, and American Society of Hypertension. *J Am Soc Hypertens* 2015;9:453–98.
- [3] Silverman MG, Blaha MJ, Krumholz HM, et al. Impact of coronary artery calcium on coronary heart disease events in individuals at the extremes of traditional risk factor burden: the Multi-Ethnic Study of Atherosclerosis. *Eur Heart J* 2014;35:2232–41.
- [4] Liu X, Gao Z, Xiong H, et al. Three-dimensional hemodynamics analysis of the circle of Willis in the patient-specific nonintegral arterial structures. *Biomech Model Mechanobiol* 2016;15:1439–56.
- [5] Wu W, Pirbhulal S, Zhang H, et al. Quantitative assessment for selftracking of acute stress based on triangulation principle in a wearable sensor system. *IEEE J Biomed Health Inform* 2018;2168–94.
- [6] Gao Z, Li Y, Sun Y, et al. Motion tracking of the carotid artery wall from ultrasound image sequences: a nonlinear state-space approach. *Trans Med Imaging* 2017;37:273–83.
- [7] Muhlestein JB, Lappé DL, Lima JA, et al. Effect of screening for coronary artery disease using CT angiography on mortality and cardiac events in high-risk patients with diabetes: the FACTOR-64 randomized clinical trial. *JAMA* 2015;312:2234–43.
- [8] Wolterink JM, Leiner T, de Vos BD, et al. Automatic coronary artery calcium scoring in cardiac CT angiography using paired convolutional neural networks. *Med Image Anal* 2016;34:123–36.
- [9] Hulten E, Bittencourt MS, Ghoshhajra B, et al. Incremental prognostic value of coronary artery calcium score versus CT angiography among symptomatic patients without known coronary artery disease. *Atherosclerosis* 2014;233:190–5.
- [10] Ghadri JR, Küest SM, Goetti R, et al. Image quality and radiation dose comparison of prospectively triggered low-dose CCTA: 128-slice dual-source high-pitch spiral versus 64-slice single-source sequential acquisition. *Int J Cardiovasc Imaging* 2012;28:1217–25.
- [11] Raju R, Thompson AG, Lee K, et al. Reduced iodine load with CT coronary angiography using dual-energy imaging: a prospective randomized trial compared with standard coronary CT angiography. *J Cardiovasc Comput Tomogr* 2014;8:282–8.
- [12] Becker CR. Cardiac CT: a one-stop-shop procedure? *Eur Radiol* 2006;16:M65–70.
- [13] Lin L, Wang Y, Yi Y, et al. Application of the low-dose one-stop-shop cardiac CT protocol with third-generation dual-source CT. *Zhongguo Yi Xue Ke Xue Yuan Xue Bao* 2017;39:34–41.
- [14] van Rosendael AR, Dimitriu-Leen AC, Bax JJ, et al. One-stop-shop cardiac CT: calcium score, angiography, and myocardial perfusion. *J Nucl Cardiol* 2016;23:1–4.
- [15] Perisinakis K, Seimenis I, Tzedakis A, et al. Personalized assessment of radiation risks from the one-stop-shop myocardial 256-slice CT examination. *Int J Cardiol* 2013;168:5267–72.
- [16] Abrahamsvan Doorn PJ, Hartmann JJ. Cardiothoracic CT: one-stop-shop procedure? Impact on the management of acute pulmonary embolism. *Insights Imaging* 2011;2:705–15.
- [17] Zhao S, Gao Z, Zhang H, et al. Robust segmentation of intima-media borders with different morphologies and dynamics during the cardiac cycle. *IEEE J Biomed Health Inform* 2017;1–1.

- [18] Gao Z, Xiong H, Liu X, et al. Robust estimation of carotid artery wall motion using the elasticity-based state-space approach. *Med Image Anal* 2017;37:1–21.
- [19] Wykrzykowska JJ, Arbab-Zadeh A, Godoy G, et al. Assessment of in-stent restenosis using 64-MDCT: analysis of the CORE-64 Multicenter International Trial. *AJR Am J Roentgenol* 2010;194:85–92.
- [20] Sharma RK, Voelker DJ, Sharma RK, et al. Coronary computed tomographic angiography (CCTA) in community hospitals: “current and emerging role”. *Vasc Health Risk Manag* 2010;6:307–16.
- [21] Mazimba S, Grant N, Parikh A, et al. Comparison of the 2006 and 2010 cardiac CT appropriateness criteria in a real-world setting. *J Am Coll Radiol* 2012;9:630–4.
- [22] Potier L, Matallali N, Moliammed K. Coronary artery disease screening using coronary computed tomography angiography. *JAMA* 2015;313:1267.
- [23] Yin WH, Lu B, Gao JB, et al. Effect of reduced X-ray tube voltage, low iodine concentration contrast medium, and sinogram-affirmed iterative reconstruction on image quality and radiation dose at coronary CT angiography: results of the prospective multicenter REALISE trial. *J Cardiovasc Comput Tomogr* 2015;9:215–24.
- [24] Rubin GD, Leipsic J, Joseph Schoepf U, et al. CT angiography after 20 years: a transformation in cardiovascular disease characterization continues to advance. *Radiology* 2014;271:633–52.
- [25] Stassi D, Dutta S, Ma H, et al. Automated selection of the optimal cardiac phase for single-beat coronary CT angiography reconstruction. *Med Phys* 2016;43:324.
- [26] So A, Imai Y, Nett B, et al. Technical note: evaluation of a 160-mm/256-row CT scanner for whole-heart quantitative myocardial perfusion imaging. *Med Phys* 2016;43:4821.
- [27] Fan L, Zhang J, Xu D, et al. CTCA image quality improvement by using snapshot freeze technique under prospective and retrospective electrocardiographic gating. *J Comput Assist Tomogr* 2015;39:202–6.
- [28] Leipsic J, Labounty TM, Hague CJ, et al. Effect of a novel vendor-specific motion-correction algorithm on image quality and diagnostic accuracy in persons undergoing coronary CT angiography without rate-control medications. *J Cardiovasc Comput Tomogr* 2012;6:164–71.
- [29] Li Q, Li P, Su Z, et al. Effect of a novel motion correction algorithm (SSF) on the image quality of coronary CTA with intermediate heart rates: segment-based and vessel-based analyses. *Eur J Radiol* 2014;83:2024–32.